Hydrothermal synthesis of zeolites from green container glass

Jenika Maisuria [1], Victoria K. Elmes [1], Andrew P. Hurt [1], Aimee A. Coleman [2], Nichola J. Coleman [1]

[1] Faculty of Engineering and Science, University of Greenwich, Chatham Maritime, Kent, ME4 4TB, UK

[2] School of Physics, University of Bristol, Bristol, BS8 1QU, UK

Corresponding author: n.coleman@gre.ac.uk (Nichola J. Coleman)

Abstract: Landfilling and stockpiling unrecycled colored container glass represents a considerable failure in sustainability with respect to the conservation of energy and mineral resources. In this study, the single-step hydrothermal synthesis of low-silica zeolites from a mixture of waste green container glass and aluminum foil (Al:Si = 1) in 4 M $NaOH_{(aq)}$ at 125 °C was followed at 1, 3, 7 and 14 days. The principal phases, sodalite and cancrinite, appeared within 1 day accompanied by minor quantities of hydrogarnet and tobermorite arising from a stoichiometric excess of calcium ions in the parent glass. Products of 63, 67, 71 and 72% crystallinity were obtained at 1, 3, 7 and 14 days, respectively, with partial successive conversion of sodalite to cancrinite over time. Ion-exchange and catalytic applications of sodalite and cancrinite arise from the high anionic charge of the 1:1 ratio of alternating SiO_4^{4-} and AlO_4^{5-} units within their aluminosilicate frameworks. In this respect, the uptake capacity of the 14-day zeolitic product for Cu^{2+} and Cd^{2+} ions (1.58 meq g^{-1} and 1.66 meq g^{-1}, respectively) was within the expected range for zeolites and compared favorably with those reported for other inorganic sorbents derived from industrial and municipal wastes. The 14-day product was also found to be an effective basic heterogeneous catalyst for the Knoevenagel condensation reaction.

Keywords: sodalite, cancrinite, container glass, Knoevenagel condensation, ion-exchange

1. Introduction

Soda-lime-silica container glass accounts for 45% of the worldwide manufacture of all glasses and typically between 30 and 70% waste cullet is included in the feedstock (Conradt, 2019). It is theoretically possible to recycle up to 90% cullet in the production of new container glass; however, many technical and economic factors give rise to considerable variation in the extent to which it is actually recycled across the globe. For example, the recycling of green and amber glass bottles is generally limited to regions with extensive brewing and wine-making industries. Container glass recycling rates in Europe, USA and Australia are reported to be 73%, 34% and 42%, respectively, with significant diversity among the various regions, states and territories (Heriyanto et al., 2018).

The production of container glass is an energy-intensive process with a substantial environmental impact (Mishra, 2015; Grbeš, 2016). Currently, the minimum energy consumption for container glass produced from 50% recycled cullet using the most efficient furnaces is estimated to be 3.85 MJ kg^{-1} (Conradt, 2019). Furthermore, despite the considerable abundance of silica in the lithosphere, the mining of sand for the production of glass is associated with catastrophic environmental problems such as erosion, flooding, land degradation, loss of biodiversity and myriad forms of pollution (Mishra, 2015). Hence, the landfilling and stockpiling of unrecycled container glass represents a considerable failure in sustainability with respect to the conservation of energy and mineral resources.

Recent initiatives to reutilize and upcycle waste container glass in the production of ceramics, geopolymers, building materials, ion-exchangers, sorbents and catalysts have been reported in the literature (Coleman et al., 2015; Silva et al., 2017; Bobirică et al., 2018; Elmes et al., 2018; Heriyanto et al., 2018; Ayala Valderrama et al., 2019; Giro-Paloma et al., 2019; Taylor et al., 2020). In particular, increasing

attention has been given to the synthesis of zeolites from waste container glass as it potentially provides a consistent source of reactive silica, irrespective of color and origin (Espejel-Ayala et al., 2014; Terzano et al., 2015; Elmes et al., 2018; Lin et al., 2019; Majdinasab and Yuan, 2019a; Majdinasab and Yuan, 2019b; Collins et al., 2020; Taylor et al. 2020). The amorphous silicate species in container glass are sufficiently reactive under mild hydrothermal conditions (typically 60 - 200 °C in 1 - 5 M alkaline hydroxide solution) to eliminate the need for pre-conditioning or activation by alkaline fusion (Terzano et al., 2015; Elmes et al., 2018). The growing interest in container glass as a feedstock for zeolite production also arises from its low concentration of potentially hazardous components (*e.g.* < 0.5 wt% of Cr_2O_3) in comparison with those of other silicate-bearing industrial and municipal wastes such as fly ashes and slags (Majdinasab and Yuan, 2019a).

The annual international market for synthetic zeolites is currently worth over 5 billion USD (Collins et al., 2020) and the use of waste feedstock materials represents potential reductions in cost, energy consumption, natural resources, landfilling, disposal and emissions. In this respect, various mixtures of zeolites have been prepared from ground container glass combined with numerous aluminum sources in alkali metal hydroxide solution under hydrothermal conditions (Espejel-Ayala et al., 2014; Terzano et al., 2015; Elmes et al., 2018; Lin et al., 2019; Majdinasab and Yuan, 2019a; Majdinasab and Yuan, 2019b; Collins et al., 2020; Taylor et al. 2020).

The present study extends the emerging body of research on waste container glass-derived zeolites by quantitatively monitoring the phase evolution of the reaction between green container cullet and waste aluminum foil (at Al:Si ~ 1) in 4 M sodium hydroxide solution at 125 °C. In addition, the potential for the zeolite product to sorb $Cu^{2+}_{(aq)}$ and $Cd^{2+}_{(aq)}$ ions and also to catalyze the industrially significant Knoevenagel reaction are investigated.

In this study, the phase assemblage and crystallinity of the hydrothermal reaction products were monitored at 1, 3, 7 and 14 days by powder X-ray diffraction analysis (XRD) with Rietveld refinement. The reaction products were also characterised by Fourier transform infrared spectroscopy (FTIR), ^{29}Si and ^{27}Al magic angle spinning nuclear magnetic resonance spectroscopy (MAS NMR) and scanning electron microscopy (SEM) with energy dispersive X-ray analysis (EDX). The catalytic activity of the 14-day zeolite product was tested on the condensation reactions between benzaldehyde and malononitrile or ethyl cyanoacetate. The respective condensation products, benzylidenemalononitrile or ethyl (2E)-2-cyano-3-phenylacrylate, and other reaction constituents were identified by gas chromatography with mass spectrometry (GC-MS) and the reaction rates in the presence and absence of the zeolite product were monitored by gas chromatography (GC). The uptake of $Cu^{2+}_{(aq)}$ and $Cd^{2+}_{(aq)}$ ions by the 14-day zeolite product was evaluated by batch sorption and compared with those of other waste-derived sorbents.

2. Materials and methods

Discarded aluminum foil and green soda-lime-silica beer and wine bottles were obtained from domestic refuse in Kent, UK. The bottles were rinsed with water to remove paper labels, ball milled and sieved to 125 µm. Quantitative oxide analysis of the green glass was obtained by X-ray fluorescence spectroscopy at the Materials Research Institute, Sheffield Hallam University, Sheffield, UK: SiO_2 - 72.15 wt%; Na_2O - 13.21 wt%; CaO - 10.48 wt%; Al_2O_3 - 1.48 wt%; MgO - 0.94 wt%; K_2O - 0.59 wt%; Fe_2O_3 - 0.46; SO_3 - 0.28 wt%; Cr_2O_3 - 0.27. All other reagents (NaOH pellets (>98%), benzaldehyde (99%), malononitrile (>99%), ethyl cyanoacetate (>98%), $Cu(NO_3)_2.2.5H_2O$ (>98%) and $Cd(NO_3)_2.4H_2O$ (>98%)) were purchased from Sigma-Aldrich, UK, and used without further purification or modification.

2.1. Hydrothermal preparation of zeolites from green container glass

The zeolites were prepared by adapting the method described by Elmes et al. (Elmes et al., 2018). In each case, an aqueous solution containing 0.9 g of aluminum foil dissolved in 60 cm^3 of 4 M $NaOH_{(aq)}$ at room temperature was mixed with 3.0 g of ground glass. The mixture was then sealed in a PTFE-lined steel autoclave and placed in a pre-heated oven at 125 °C. A total of 12 samples of the same composition were prepared individually. After 1 day, three autoclaves were removed from the oven and cooled in air to room temperature before opening. The solid products were then recovered by gravitational filtration, washed with deionised water to pH 8 and dried to constant mass in air at 60 °C

(for ~3 days) prior to analysis. Similarly three samples were also recovered, washed and dried after 3, 7 and 14 days. Samples prepared at 1, 3, 7 and 14 days were labelled ZEO-1, ZEO-3, ZEO-7 and ZEO-14, respectively.

2.2. Characterisation of zeolite products

The ground green glass and reaction products were analysed by powder XRD using a Bruker D8 diffractometer with Cu Kα = 1.5406 Å, a step size of 0.019 ° in the 2θ range from 5 to 60 ° and a measuring time of 1 s per step. The weight fractions of the crystalline phases were determined by Rietveld refinement using Bruker TOPAS version 5.0 software. FTIR spectra were obtained using a Perkin Elmer Spectrum Two spectrometer between 500 and 2000 cm^{-1} wavenumbers, with 10 scans at a resolution of 4 cm^{-1}. Secondary electron images of the products were acquired from uncoated samples attached to carbon tabs on an Hitachi SU8030 scanning electron microscope with an accelerating voltage of 1 kV. EDX data were collected in quintuplicate from areas of approximately 100 μm^2 using a JEOL JSM-5410 LV electron microscope with an Oxford Instruments X-MaxN EDX detector in low vacuum mode with an accelerating voltage of 8 kV. The specific surface areas of the ground green glass and 14-day reaction product (ZEO-14) were estimated by nitrogen gas sorption analysis via the BET method using a Micromeritics Gemini VII gas sorption analyser (Coleman and Hench, 2000). Prior to analysis, the samples were degassed overnight at 80 °C under flowing nitrogen. BET isotherms were collected in duplicate for both samples. MAS NMR spectra of the green glass and ZEO-14 product were collected on a JEOL JNM-ECX 300 MHz spectrometer. Single pulse ^{29}Si MAS NMR spectra were obtained with a pulse delay of 60 s, an acquisition time of 0.02048 s and a minimum of 25 000 scans. Single pulse ^{27}Al MAS NMR spectra were collected with a pulse delay of 0.5 s, an acquisition time of 0.01024 s and 8000 scans. ^{29}Si and ^{27}Al chemical shifts were referenced to tetramethylsilane and the aluminum hexaquo ion $[Al(H_2O)_6]^{3+}$, respectively.

2.3. Catalysis of the Knoevenagel condensation reaction

The basic catalytic properties of the ZEO-14 product were evaluated using the reaction between benzaldehyde and malononitrile or ethyl cyanoacetate to produce benzylidenemalononitrile or ethyl (2E)-2-cyano-3-phenylacrylate, respectively. Mixtures of benzaldehyde (19 mmol) and malononitrile (19 mmol) or ethyl cyanoacetate (19 mmol) in 50 cm^3 of ethanol, were heated at 50 °C under reflux with constant stirring. At 15 and 60 min, 1 cm^3 aliquots of the reaction mixture were analysed by GC, using an Agilent 7683B instrument with either an HP-1 or DB-5 capillary column for the respective detection of benzylidenemalononitrile or ethyl (2E)-2-cyano-3-phenylacrylate by flame ionisation. The condensation products and other reaction constituents were confirmed by GC-MS using a Perkin Elmer turbomass DB5 spectrometer. The same reactions were also conducted in the presence of 0.25 g of ZEO-14. All reactions were carried out in triplicate. The relative peak areas of the reaction products in the GC chromatogram were used to represent the extent of reaction and plotted as a function of time. The relative initial rate of reaction was estimated from the ratio of the initial gradient of the plot in the presence and absence of ZEO-14.

2.4. Uptake of Cu^{2+} and Cd^{2+} ions

The removal of Cu^{2+} and Cd^{2+} ions from aqueous solutions by the ZEO-14 product was determined in triplicate by single metal batch sorption. In each case, 0.10 g of ZEO-14 was contacted with 0.2 dm^3 of metal nitrate solution at a concentration of 0.5 mM in a polypropylene bottle at 25 °C. After 24 h, the supernatant liquors were recovered by centrifugation at 3000 rpm and analyzed by inductively coupled plasma spectroscopy (ICP) using a TJA Iris simultaneous ICP-OES spectrophotometer.

3. Results and discussion

3.1. Characterisation of the zeolite products

Powder XRD patterns of the ground green container glass (GCG) and zeolite products are shown in Fig. 1. The compositions of the reaction products are listed in Table 1 and the development of the phase assemblage is plotted in Fig. 2. These XRD data indicate that, under the selected reaction conditions,

approximately 63% of the amorphous glass is transformed into crystalline product phases within 1 day. The subsequent conversion of the glass is incremental with ~67, 71 and 72% crystallinity being achieved by 3, 7 and 14 days, respectively (Table 1, Fig. 2).

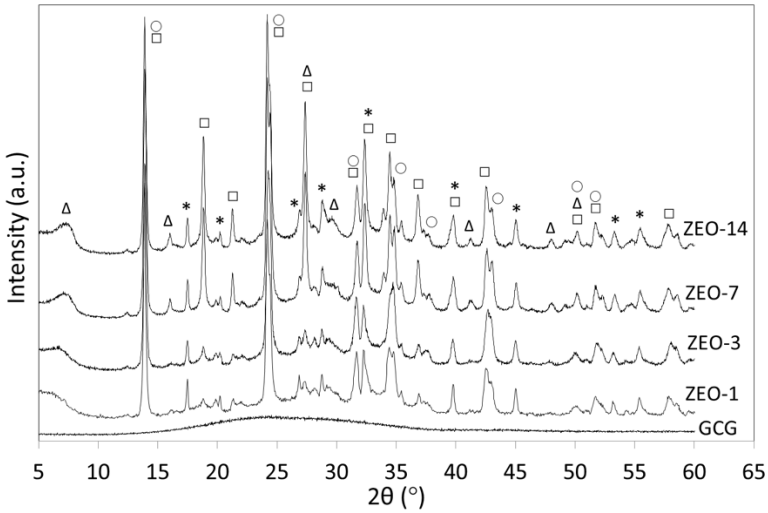

Fig.1. XRD patterns of green container glass (GCG) and hydrothermal products synthesized for 1, 3, 7 and 14 days in 4 M $NaOH_{(aq)}$ (viz. ZEO-1, ZEO-3, ZEO-7 and ZEO-14, respectively) at 125 °C
Key: ○ - sodalite; □ - cancrinite; * - katoite; Δ - tobermorite

Table 1. Compositions of the hydrothermal reaction products

Phase	**ZEO-1**	**ZEO-3**	**ZEO-7**	**ZEO-14**
Sodalite (PDF 041-0009) (%)	38.38	40.09	37.46	29.98
Cancrinite (PDF 075-5322) (%)	11.70	12.68	20.22	23.92
Katoite (PDF 077-1713) (%)	8.59	9.34	8.79	9.99
Tobermorite (PDF 045-1480) (%)	4.00	4.18	4.26	7.51
Calcite (PDF 005-0586) (%)	0.19	0.41	0.58	0.96
Crystallinity (%)	62.9 ± 1.4	66.5 ± 1.4	71.2 ± 2.1	72.1 ± 1.7
Weighted profile R-factor (R_{wp})	9.42	7.78	10.07	11.53

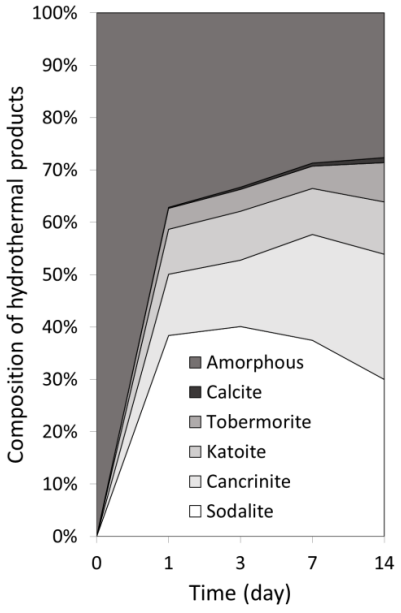

Fig. 2. The phase evolution of the hydrothermal products synthesized for 1, 3, 7 and 14 days

The principal product after 1 day is sodalite which continues to develop up to 3 days and is then partially replaced by cancrinite at longer reaction times. Sodalite and cancrinite are ultramicroporous low-silica zeolites whose naturally-occurring analogues are members of the feldspathoid family of minerals (Ríos Reyes et al., 2013). They share a common chemical formula, $Na(Al_6Si_6O_{24}).2NaX.6H_2O$, where X is typically Cl^-, OH^-, NO_3^-, $0.5CO_3^{2-}$ or $0.5SO_4^{2-}$; although, they are composed of different structural 3-D aluminosilicate frameworks. In this instance, the principal non-framework anion is OH^-, with minor substitutions of CO_3^{2-} expected from atmospheric carbonation of the alkaline reaction mixture. Atmospheric carbonation also gives rise to trace quantities of calcite below 1 wt% (Table 1).

Zeolites prepared from solid particulate parent materials under mild hydrothermal conditions form via a dissolution, nucleation and growth mechanism. During this type of synthesis, after nucleation, a series of transitory thermodynamically-metastable intermediate phases evolves according to the Ostwald Law of Successive Transformations (Cundy and Cox, 2005). The initial precipitation of sodalite and its subsequent conversion to cancrinite, as observed in the present study, is a commonly acknowledged sequential reaction in sodium hydroxide solution of approximately equimolar concentrations of AlO_4^{5-} and SiO_4^{4-} species (Ríos Reyes et al., 2013). The presence of calcium ions (arising from the green glass in this instance) is reported to promote the transformation of sodalite to cancrinite, as the latter structure tolerates greater substitution of Na^+ by Ca^{2+} during precipitation (with a maximum replacement of two Na^+ ions per unit formula) (Xu et al., 2010).

The hydrogarnet, katoite ($Ca_3Al_2(SiO_4)(OH)_8$), is consistently present among the reaction products at approximately 9 wt% in all samples and the poorly crystalline layer-lattice tobermorite phase ($Ca_5Si_6O_{16}(OH)_2.4H_2O$) appears in increasing proportions up to 7.5 wt% within 14 days (Fig. 2, Table 1). These phases arise from an excess of Ca^{2+} ions in the parent glass with respect to the upper limit of substitution of this ion in the sodalite and cancrinite structures during formation. It should be noted, that the post-synthesis replacement (i.e. ion-exchange) of the non-framework cations in both sodalite and cancrinite is significantly more extensive than that during their formation and underpins the basis of their industrial applications as sorbents for a wide range of heavy metal species.

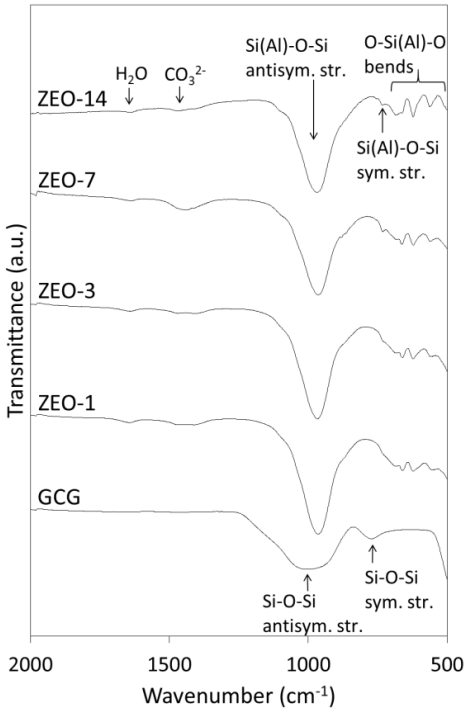

Fig. 3. FTIR spectra of green container glass (GCG) and hydrothermal products

FTIR spectra of the ground green container glass (GCG) and hydrothermal zeolite products are shown in Fig. 3. The spectrum of the green glass comprises a very broad asymmetrical signal circa 1000 cm^{-1} arising from the antisymmetric stretching of the polymerized Si-O-Si network of the glass; and the

less intense band centered at 770 cm^{-1} is attributed to symmetric stretching modes within the amorphous Si-O-Si system (El Batal et al., 2017).

Following hydrothermal processing, the main antisymmetric Si-O-Si stretching band narrows, intensifies and shifts to 970 cm^{-1} as the amorphous silicate network is replaced by the crystalline Si(Al)-O-Si framework system of the zeolite products (Fig. 3) (Elmes et al., 2018). The symmetric stretching band of the Si(Al)-O-Si framework at 735 cm^{-1} and signals arising from the various O-Si(Al)-O bending modes at 665 cm^{-1}, 625 cm^{-1} and 565 cm^{-1} are initially poorly defined and become sharper, more intense and better resolved as crystallinity increases with reaction time (Elmes et al., 2018).

Bending vibrations of water and hydroxyl groups are noted at approximately 1645 cm^{-1} and carbonate ion stretching of calcite gives rise to the band at 1450 cm^{-1} in the spectra of the products (Fig. 3) (Elmes et al., 2018). Individual signals arising from the minor katoite and tobermorite phases are not observed in the FTIR spectra of the hydrothermal products as these are obscured by the various more intense lattice vibrations of the principal sodalite and cancrinite phases.

The ^{29}Si MAS NMR spectra of the ground green container glass and 14-day hydrothermal product, ZEO-14, are shown in Fig. 4(a). Solid state ^{29}Si MAS NMR spectroscopy is used to identify the degree of polymerization and local chemical environment of silicate species in glasses and mineral phases (Engelhardt and Michel, 1987). Notation used to describe the silicate environments is such that the symbol Q represents one SiO_4^{4-} tetrahedron and the superscript, n, denotes the number of other Q units to which it is bonded via Si-O-Si linkages. SiO_4^{4-} tetrahedra bonded to AlO_4^{5-} units (via Si-O-Al linkages) are denoted as $Q^n(mAl)$, where m is the number of AlO_4^{5-} units. For example, a midchain SiO_4^{4-} unit linked to two other SiO_4^{4-} units is represented as Q^2, and a fully polymerized SiO_4^{4-} unit linked to two other SiO_4^{4-} units and two AlO_4^{5-} units is represented as $Q^4(2Al)$.

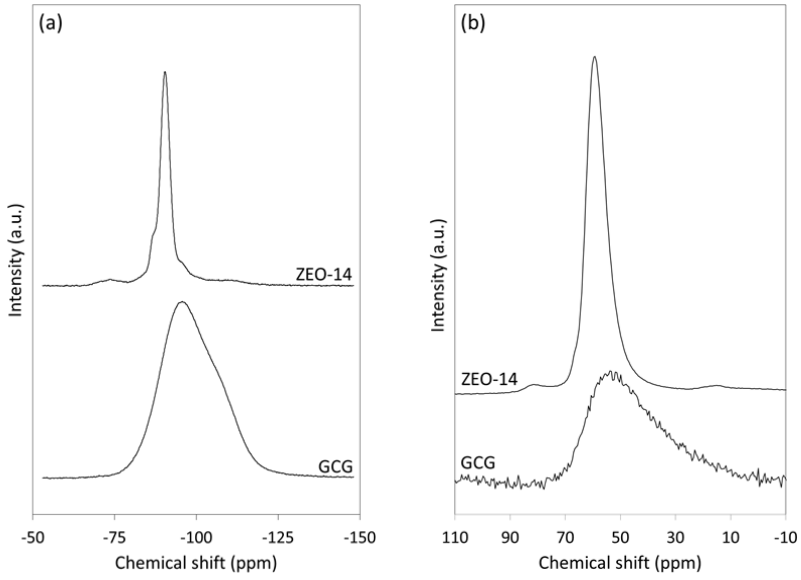

Fig. 4. (a) ^{29}Si and (b) ^{27}Al MAS NMR spectra of green container glass (GCG) and hydrothermal products synthesized for 14 days in 4 M $NaOH_{(aq)}$ at 125 °C

The ^{29}Si MAS NMR spectrum of the green glass presents a single extremely broad asymmetrical resonance with maximum intensity at approximately -95 ppm (Fig. 4(a)). The observed signal is consistent with various amorphous Q^2-Q^4 silicate units in the chemical shift range between -80 and -110 ppm comprising a predominance of Q^3 species, as would be expected for a melt-derived soda-lime-silica glass (Coleman, 2011).

The principal contribution to the compound asymmetrical signal at -88 ppm in the ^{29}Si MAS NMR spectrum of the ZEO-14 hydrothermal product is the $Q^4(4Al)$ silicate system of sodalite and cancrinite (Fig. 4(a)) (Mashal et al., 2005). This unresolved resonance is characteristic of the alternating SiO_4 and AlO_4 units within the framework lattices of both sodalite and cancrinite. The upfield shoulder at approximately -83 ppm arises from the various Q^2 and $Q^2(1Al)$ species of tobermorite and also from the silicate centers in katoite that are linked to four octahedral aluminate units (Pena et al., 2008). Residual

unreacted parent glass gives rise to the downfield shoulder at ~ -95 ppm and the broad resonance circa -73 ppm is tentatively assigned to a calcium/sodium aluminosilicate gel phase (Taylor et al., 2020). It was not possible to deconvolute the ^{29}Si MAS NMR spectrum of ZEO-14 owing to the poorly defined resonance arising from the residual glass and lack of information on the relative intensities of the Q^1, Q^2, Q^2(1Al) and Q^3 environments in the tobermorite phase. In this respect, ^{29}Si MAS NMR analysis generated limited additional information to that obtained by XRD and FTIR for this system. Accordingly, owing to the cost and time-consuming nature of this technique, the other hydrothermal reaction products, ZEO-1, ZEO-3 and ZEO-7 were not analysed by MAS NMR spectroscopy.

The ^{27}Al MAS NMR spectra of the ground green container glass and 14-day hydrothermal product, ZEO-14, are shown in Fig. 4(b). Solid state ^{27}Al MAS NMR spectroscopy is used to determine the coordination environment of aluminum species in glasses and minerals. Octahedral aluminum gives rise to resonances in the chemical shift range 20 to −10 ppm, and tetrahedrally-coordinated aluminum species appear between 100 and 50 ppm (Engelhardt and Michel, 1987).

The ^{27}Al MAS NMR spectrum of the green container glass comprises one very broad resonance of maximum intensity at approximately 54 ppm that arises from the highly disorganized tetrahedral aluminum species within the amorphous glass system (Fig. 4(b)). The signal-noise ratio of this spectrum is low, despite the collection of 8 000 scans, as the aluminum concentration is lower <1 wt%.

The asymmetrical resonance at ~60 ppm in the ^{27}Al MAS NMR spectrum of ZEO-14 is assigned to the tetrahedral aluminate species within the sodalite and cancrinite frameworks (Mashal et al., 2005). This signal obscures those of the tetrahedral bridging (~65 ppm) and branching (~60 ppm) aluminum species substituted into the tobermorite lattice that are expected to appear as an unresolved signal in that region of the spectrum (Houston et al., 2009). The resonance at 14 ppm arises from octahedral aluminum in katoite (Pena et al., 2008); and the signal at 80 ppm is tentatively assigned to tetrahedral $Al(OH)_4^-$ species within the calcium/sodium aluminosilicate gel phase which may also be present as extra-framework anions associated with the sodalite and cancrinite phases (Graham et al., 2018).

Secondary electron SEM images of the ground green container glass and hydrothermal products are shown in Fig. 5. Scanning electron microscopy indicates that the ground green glass consists of angular irregularly-shaped fragments generally below 100 µm in diameter with a large quantity of particles below 10 µm (Fig. 5). Hydrothermal processing of the green glass under the selected reaction conditions results in granular products of varying aspect ratio and broad particle size distribution up to approximately 1 mm in length (Fig. 5). The initial precipitation of the products is seen to form concretions in which the residual partially eroded glass fragments are embedded. This is most clearly observed in the image of ZEO-3 with the 500 µm scale-bar in Fig. 5.

In many industrial applications, it is necessary to convert fine zeolite powders into granular materials to improve mechanical properties, to optimize mass and/or heat transfer and for ease of handling and separation (Bingre et al., 2018). This is achieved by combining the zeolite powders with temporary or permanent binders to 'shape' the zeolites, which adds to the cost and complexity of processing and can also have a detrimental impact on the desirable properties of the zeolites (e.g. acidity, surface area and porosity). The direct production of granular zeolitic products rather than finely dispersed powdered zeolites may present an advantageous reduction or elimination in the need to use binders in certain applications.

The surface of the initial 1-day product (ZEO-1) is entirely populated with lepispherical ball-of-wool morphologies between 5 and 10 µm in diameter that are characteristic of sodalite (Ríos Reyes et al., 2013). Dispersed across the surface of this product are also some smaller (~2 µm) globular deposits that disappear within 3 days and are considered to be a calcium/sodium aluminosilicate gel precursor to the sodalite phase (Fig. 5). As the reaction progresses, the sodalite structures grow up to 20 and 40 µm in diameter between 3 and 14 days, and fine foliaceous deposits of tobermorite are observed to be distributed across the surface by 7 days (Fig. 5) (Coleman, 2006). Some of the lepispherical sodalite structures also become infilled and repopulated by hexagonal cancrinite rods (Deng et al., 2006) within 14 days (bottom right image in Fig. 5). Despite the intimacy of these phases, it should be noted that this successive replacement of sodalite by cancrinite is known to take place via dissolution and re-precipitation, rather than by the direct interconversion of the two phases (Xu et al., 2010).

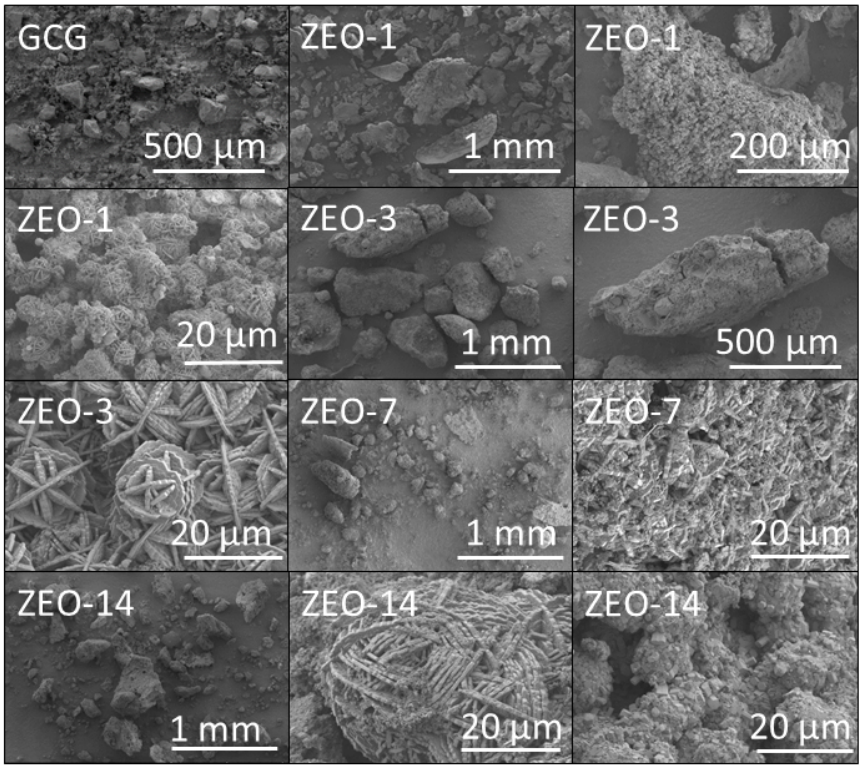

Fig. 5. Secondary electron SEM images of the ground green container glass (GCG) and hydrothermal products

Table 2. Molar elemental compositions of green container glass and hydrothermal products

Element (mol%)	GCG	ZEO-1	ZEO-3	ZEO-7	ZEO-14
Si	19.8 ± 3.2	10.6 ± 2.1	10.5 ± 0.8	9.9 ± 0.6	11.6 ± 1.2
Al	0.5 ± 0.1	6.6 ± 0.9	8.6 ± 0.5	7.9 ± 1.4	11.5 ± 0.9
Na	7.7 ± 1.0	12.0 ± 2.0	9.7 ± 0.8	11.2 ± 1.7	12.0 ± 1.7
Ca	3.1 ± 0.6	0.2 ± 0.1	0.6 ± 0.4	0.8 ± 0.2	2.1 ± 1.6
Mg	0.5 ± 0.1	0.1 ± 0.1	0.1 ± 0.1	0.1 ± 0.1	0.2 ± 0.1
C	2.5 ± 1.0	2.4 ± 1.7	1.8 ± 0.9	2.1 ± 1.1	2.5 ± 2.0
K	0.2 ± 0.1	b.d.l.	b.d.l.	b.d.l.	b.d.l.
Fe	0.1 ± 0.1	b.d.l.	b.d.l.	b.d.l.	0.1 ± 0.1
Cr	0.1 ± 0.1	b.d.l.	b.d.l.	b.d.l.	0.2 ± 0.1

Key: b.d.l. = below detection limit

Molar elemental compositions of the green glass and hydrothermal products, obtained by EDX analysis, are listed in Table 2. The Al:Si ratio of the products increases with time as the zeolite phases develop, and within 14 days, this value reflects the stoichiometry of the initial feedstock materials (i.e. Al:Si ~ 1). The concentration of Ca decreases markedly within the first day as the parent glass dissolves and the zeolite phases form. It then rises steadily with time as the proportions of tobermorite, calcite and cancrinite increase. Carbon, arising from atmospheric carbonation and also a contribution from the carbon tabs upon which the samples were mounted, was detected at, or below, 2.5 mol%. Trace quantities of Mg were present at, or below, 0.2 mol%, and the concentrations of K, Fe and Cr were generally below the detection limit of the instrument (and not greater than 0.2 mol%).

The BET external surface area of the ground green glass was initially found to be below the measurement limit of the instrument (i.e. approximately 0.5 $m^2 g^{-1}$) and increased to 5.9 ± 0.2 $m^2 g^{-1}$ after 14 days of hydrothermal treatment. It should be noted that, in this case, the BET surface area measurement of ZEO-14 refers exclusively to the external surface of the material. Under the available degassing and analysis conditions, the failure of nitrogen to effectively penetrate the ultramicropores of the sodalite and cancrinite phases prevents the measurement of the internal surface area and porosity

(Cychosz et al., 2006). Since this technique is not able to determine the internal surface area, pore size distribution and porosity of these ultramicroporous materials, the other products, ZEO-1, ZEO-3 and ZEO-7 were not analysed by nitrogen gas sorption.

3.2. Catalysis of the Knoevenagel condensation reaction

In this study, the potential of the green glass-derived 14-day hydrothermal product, ZEO-14, to catalyze the Knoevenagel condensation was tested on the reactions between benzaldehyde and malononitrile or ethyl cyanoacetate to produce benzylidenemalononitrile or ethyl (2E)-2-cyano-3-phenylacrylate, respectively. The reaction profiles in the absence and presence of ZEO-14 are plotted in Fig. 6 along with the relative initial reaction rates. These data indicate that the glass-derived zeolitic product significantly enhances the rates of both condensation reactions.

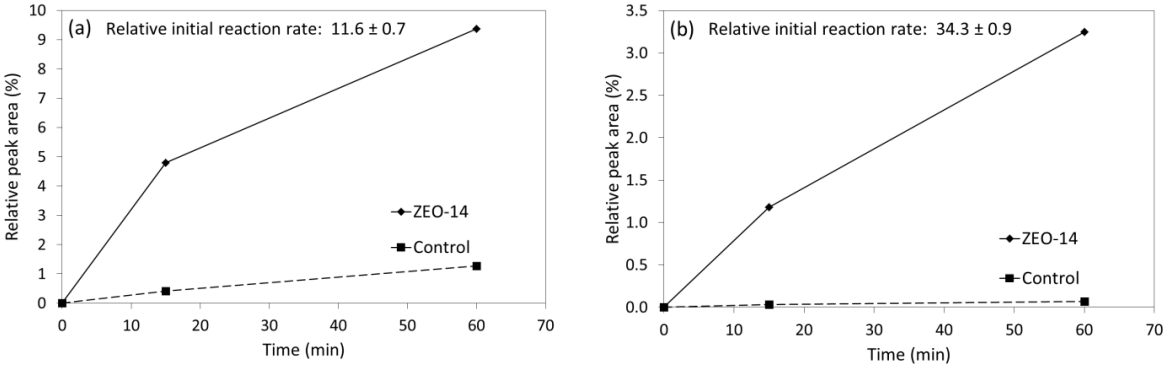

Fig. 6. Reaction profiles of (a) benzylidenemalononitrile and (b) ethyl (2E)-2-cyano-3-phenylacrylate in the absence and presence of ZEO-14.

The relevance of the Knoevenagel condensation reaction arises from its wide application in the fine chemical and pharmaceutical industries to form new carbon-carbon bonds (Jain et al., 2012). This reaction involves the condensation of an aldehyde or ketone with an activated methylene group in solution to form an unsaturated C=C product in the presence of a weak organic base. Traditionally, the Knoevenagel reaction is catalyzed homogeneously with various bases such as amines, ammonium salts and piperidine; although, heterogeneous catalysis using solid bases offers the potential to improve product separation, reduce the volume of caustic effluent, suppress side-reactions and eliminate self-condensation of the carbonyl reagent (Jain et al., 2012). In this respect, a number of recent studies has been carried out to evaluate a range of waste-derived basic metallosilicates (including zeolites, lithium metasilicate, tobermorite, hydrotalcite and hydrocalumite) as catalysts for the Knoevenagel condensation (Kuwahara et al., 2012; Ng et al., 2015; Elmes et al., 2018).

In the absence of ZEO-14, the condensation of benzaldehyde and malononitrile proceeds more rapidly than that of benzaldehyde and ethyl cyanoacetate owing to the superior electron-withdrawing capacity of the cyano group relative to that of the ester (Fig. 6). Electron-withdrawing groups facilitate the rate-determining deprotonation of the methylene group to form the carbanion which subsequently attacks the carbonyl group of the benzaldehyde (Jain et al., 2012). The observed catalytic effect of ZEO-14 is more pronounced in the latter case, despite the presence of the bulkier ester group of ethyl cyanoacetate, indicating that the basic sites of ZEO-14 are readily available to engage in the abstraction of the methylene proton (Jain et al., 2012). According to Lowenstein's rule, which forbids the formation of direct Al-O-Al bonds, sodalite and cancrinite both possess the maximum possible Al:Si ratio (i.e. unity) of any zeolite structure which confers their frameworks with the highest possible concentration and distribution of basic sites. During these Knoevenagel reactions, the interior of the sodalite and cancrinite frameworks is not accessible via the ultrafine micropores of maximum diameter ~2.2 and ~6.6 Å, respectively, and hence, the catalytic effect relies on the presentation and reactivity of the basic sites on the external surfaces (Xu et al., 2010). Tobermorite, which is present at ~7.5 wt% in ZEO-14, is also reported to catalyze the Knoevenagel condensation (Elmes et al., 2018).

In the case of all condensation reactions carried out in this study, benzoic acid was present at approximately 0.005% as an impurity in the benzaldehyde reagent. Ethyl (2Z)-2-cyano-3-

phenylacrylate, the more sterically-hindered isomer of the principal condensation product of benzaldehyde and ethyl cyanoacetate was also formed in the presence and absence of the ZEO-14 catalyst at a constant Z:E isomer ratio of 0.21. No other products were formed in any of the reaction systems. In this respect, ZEO-14 is sufficiently basic to catalyze the Knoevenagel reaction without causing the self-condensation of benzaldehyde and it neither promotes nor suppresses the formation of the Z-isomer.

A similar glass-derived product of 46% crystallinity comprising an unquantified mixture of cancrinite, sodalite, tobermorite and katoite is reported to effectively catalyze the condensation of benzaldehyde and ethyl cyanoacetate at 80 °C with a relative initial reaction rate of 16.3 (Elmes et al., 2018). The superior catalytic effect observed in the present study is principally attributed to the higher degree of crystallinity of ZEO-14.

3.3. Uptake of Cu^{2+} and Cd^{2+} ions

Divalent copper and cadmium ions were selected as model contaminants in this study to evaluate the sorptive properties of the ZEO-14 product. Cu^{2+} and Cd^{2+} ions are among the most common metal contaminants in aqueous industrial effluents and largely arise from mining and metallurgical activities (Jaishankar et al., 2014). Copper is an essential trace element that can accumulate to toxic concentrations in plant and animal species as a result of anthropogenic pollution, and cadmium is a non-essential carcinogen that exerts toxicity via a wide range of mechanisms (Festa and Thiele, 2011).

The uptakes of Cu^{2+} and Cd^{2+} ions by ZEO-14 from single metal ion solutions under batch sorption are compared with those of other waste-derived inorganic sorbents in Table 3. The sorption capacity of ZEO-14 is seen to appear in the middle of this range. Tobermorite and amorphous calcium/sodium aluminosilicate gel phases present within ZEO-14 are also anticipated to contribute to the cation-exchange capacity (Coleman et al., 2015; Javadian et al., 2015). Following exposure to ZEO-14, the pH of the supernatant copper nitrate solution was found to increase from 4.22 ± 0.05 to 5.0 ± 0.1 and that of the cadmium nitrate solution also rose from 5.41 ± 0.05 to 5.8 ± 0.2. Modest increases in supernatant pH, such as those observed here, are expected during the exchange of acidic transition metal cations for alkali metal ions and are indicative of an ion-exchange mechanism. Nonetheless, complex formation at the surface and precipitation may also be instrumental in the uptake of Cu^{2+} and Cd^{2+} by ZEO-14.

Table 3. Uptake of Cu^{2+} and Cd^{2+} by ZEO-14 and other waste-derived inorganic sorbents

Sample	Cu^{2+}-uptake (mmol g^{-1})	Cd^{2+}-uptake (mmol g^{-1})	Reference
ZEO-14	0.79 ± 0.16	0.83 ± 0.08	-
Blast furnace sludge	0.372	0.090	De Gisi et al., 2016
Red mud	0.310	0.094	De Gisi et al., 2016
Concrete fines	0.551	-	Coleman et al., 2005
Zeolite A (fly ash)	-	1.647	Izidoro et al., 2013
Cancrinite (fly ash)	2.081	-	Qiu and Zheng, 2009
Modified fly ash	2.188	1.388	Visa and Chelaru, 2014
Sewage sludge ash	0.11	0.07	Wang et al., 2019
Tobermorite (glass)	-	3.923	Coleman et al., 2014
Geopolymer (fly ash)	-	0.231	Javadian et al., 2015

3.4. Waste container glass for the synthesis of zeolites

As previously stated, landfilling and stockpiling unrecycled soda-lime-silica container glass represents a considerable failure in sustainability considering the extensive energy-consumption and environmental impact associated with its manufacture and distribution (Mishra, 2015; Grbeš, 2016; Conradt, 2019). In response to this problem, recent research has been carried out to synthesize zeolites from flint, amber and green container glasses under various alkaline hydrothermal conditions (Espejel-Ayala et al., 2014; Terzano et al., 2015; Elmes et al., 2018; Lin et al., 2019; Majdinasab and Yuan, 2019a; Majdinasab and Yuan, 2019b; Collins et al., 2020; Taylor et al. 2020). The impact of reaction composition

and temperature has been investigated in a number of previous studies (Terzano et al., 2015; Majdinasab and Yuan, 2019a; Majdinasab and Yuan, 2019b); although, to date, little consideration has been given to the kinetics of evolution of the zeolitic phase assemblage (Taylor et al., 2020) and less still to the evaluation of the properties of the glass-derived products with respect to their potential technical applications.

A recent study reports that a product of 63% crystallinity comprising a mixture of sodalite and cancrinite, with minor proportions of katoite and tobermorite, was synthesized within 10 days from amber container glass and aluminum foil in 4 M $NaOH_{(aq)}$ at 100 °C (Taylor et al., 2020). The present work confirms that the same phases arise from green container glass, owing to the comparable composition and reactivity of all soda-lime-silica container glass irrespective of color. This present work also demonstrates that products of similar crystallinity can be achieved within 1 day rather than 10 days at an increased reaction temperature of 125 °C. The higher reaction temperature and shorter reaction time also increase the proportion of sodalite relative to cancrinite in the product.

In the absence of templating agents or pre-conditioning steps, the one-pot hydrothermal synthesis of phase-pure zeolites of high crystallinity from container glass is not possible owing to the presence of 5-10 wt% CaO which limits the formation of open aluminosilicate framework structures that do not tolerate Ca^{2+} substitution during crystallization (Elmes at al., 2018; Taylor et al., 2020). This restricts the use of container glass in direct single-step hydrothermal synthesis to the production of small pore zeolites such as sodalite, cancrinite and analcime, with impurities of other hydrated calcium aluminosilicate phases such as tobermorite, katoite and calcium/sodium aluminosilicate gel. This is not necessarily disadvantageous, as mixtures of impure zeolitic phases are acceptable in many low-grade industrial and agricultural applications. In fact, the presence of Ca^{2+} ions in container glass has been successfully exploited by Takei et al. (Takei et al., 2012) to produce a foamed porous composite of zeolite P, analcime and residual glass particles that was consolidated by the precipitation of calcite ($CaCO_3$) during a direct one-step hydrothermal treatment of the glass in 0.2 M $Na_2CO_{3(aq)}$ at 150 °C.

Additional pre-conditioning and processing stages are optional and could be implemented on a value-added basis to obtain a wider range of more refined zeolite products. For example, acid-leaching or complexing with ligands could be used to remove calcium ions and enrich the silica-content of the glass, although such strategies would increase the effluent stream and cost of processing. Similarly, templating agents are not required for the hydrothermal preparation of zeolites from waste container glass; although, the synthesis of larger pore zeolites such as ZSM-5 from a mixture of glass and paper sludge ash has been demonstrated using a tetrapropilammonium bromide template (Espejel-Ayala et al., 2014). Inevitably, the physicochemical properties and potential applications of container glass-derived zeolites will ultimately determine the economic feasibility of including any additional processing steps or incorporating fine chemical regents.

In order to reduce the energy and time required to generate zeolites from waste container glass, their synthesis under microwave irradiation has recently been proposed (Majdinasab and Yuan, 2019a; Majdinasab and Yuan, 2019b). The preparation of container glass-derived zeolite A at room temperature has also been demonstrated, although only 15% crystallinity was achieved after 180 days from a mixture of 8 g glass and 0.5 g aluminum alloy in 80 cm^3 of 2.5 M $NaOH_{(aq)}$. The modest temperature range in which the preparation of zeolites from waste container glass is reported (i.e. generally between 60 and 200 °C) also offers the possibility to synthesize these materials using recovered heat generated from other higher temperature industrial processes (Jouhara et al., 2018).

The present study has demonstrated that an impure mixture of sodalite and cancrinite can be produced from waste glass and aluminum that has the potential to be used as a basic catalyst or cation-exchange substrate. Further work is warranted to more fully explore potential options for the energy-efficient synthesis of zeolites from waste container glass and the scaling-up of the processes should also be considered.

4. Conclusions

This study has confirmed that an impure mixture of sodalite and cancrinite can be produced from ground green container glass and dissolved waste aluminum (Al:Si = 1) in 4 M $NaOH_{(aq)}$ at 125 °C. A granular product of 63% crystallinity comprising a mixture of sodalite and cancrinite, with minor

proportions of katoite and tobermorite, forms within 1 day. Crystallinity increases to 72% within 14 days and is accompanied by partial replacement of sodalite to cancrinite over time. Despite the incomplete crystallization of green glass into zeolitic phases, the uptake capacity of the 14-day product for Cu^{2+} and Cd^{2+} ions compared favorably with those of other inorganic sorbents derived from industrial and municipal wastes. The 14-day product was also found to be an effective basic heterogeneous catalyst for the Knoevenagel condensation reaction.

References

AYALA VALDERRAM, D.M., GÓMEZ CUASPUD, J.A., ROETHER, J.A., BOCCACCINI, A.R., 2019. *Development and characterization of glass-ceramics from combinations of slag, fly ash, and glass cullet without adding nucleating agents*. Materials 12, 2032.

BINGRE, R., LOUIS, B., NGUYEN, P., 2018. *An overview on zeolite shaping technology and solutions to overcome diffusion limitations*. Catalysis, 8, 163.

BOBIRICĂ, C., SHIM, J.-H., PARK, J.-Y., 2018. *Leaching behavior of fly ash-waste glass and fly ash-slag-waste glass-based geopolymers*. Ceram. Int. 44, 5886-5893.

COLEMAN, N.J., LEE, W.E., SLIPPER, I.J., 2005. *Interactions of aqueous Cu^{2+}, Zn^{2+} and Pb^{2+} ions with crushed concrete fines*. J. Hazard. Mater. B121, 203-213.

COLEMAN, N.J., HENCH, L.L., 2000. *A gel-derived mesoporous silica reference material for surface analysis by gas sorption 1. Textural features*. Ceram. Int. 26, 171-178.

COLEMAN, N.J., 2006. *Interactions of Cd(II) with waste-derived 11 Å tobermorites*. Sep. Purif. Technol. 48, 62-70.

COLEMAN, N.J., 2011. *11 Å tobermorite ion exchanger from recycled container glass*. Int. J. Environ. Waste Manage. 8, 366-382.

COLEMAN, N.J., LI, Q., RAZA, A. 2014. *Synthesis, structure and performance of calcium silicate ion exchangers from recycled container glass*. Physicochem. Probl. Miner. Process. 50, 5-16.

COLEMAN, N.J., HURT, A.P., RAZA, A., 2015. *Hydrothermal synthesis of lithium silicate (Li_2SiO_3) from waste glass: a preliminary stu*dy. Physicochem. Probl. Miner. Process. 51, 685-694

COLLINS, F., ROZHKOVSKAYA, A., OUTRAM, J.G., MILLAR, G.J., 2020. *A critical review of waste resources, synthesis, and applications for Zeolite LTA*. Microporous Mesoporous Mater. 291, 109667.

CONRADT, R., 2019. *Prospects and physical limits of processes and technologies in glass melting*. J. Asian Ceram. Soc. 7, 377-396.

CUNDY, C.S., COX, P.A., 2005. *The hydrothermal synthesis of zeolites: precursors, intermediates and reaction mechanism*. Microporous Mesoporous Mater. 82, 1-78.

CYCHOSZ, K.A., GUILLET-NICOLAS, R., GARCÍA-MARTÍNEZ, J., THOMMES, M., 2017. *Recent advances in the textural characterization of hierarchically structured nanoporous materials*. Chem. Soc. Rev. 46, 389-414.

DE GISI, S., LOFRANO, G., GRASSI, M., NOTARNICOLA, M., 2016. *Characteristics and adsorption capacities of low-cost sorbents for wastewater treatment: A review*. Sustain. Mater. Technol. 9, 10-40.

DENG, Y., FLURY, M., HARSH, J.B., FELMY, A.R., QAFOKUB, O., 2006. Cancrinite and sodalite formation in the presence of cesium, potassium, magnesium, calcium and strontium in Hanford tank waste simulants. Appl. Geochem. 21, 2049-2063.

EL BATAL, H.A.; HASSAAN, M.Y., FANNY, M.A., IBRAHIM, M.M., 2017. *Optical and FT infrared absorption spectra of soda lime silicate glasses containing nano Fe_2O_3 and effects of gamma irradiation*. Silicon 9, 511-517.

ELMES, V.K., EDGAR, B.N., MENDHAM, A.P., COLEMAN, N.J., 2018. *Basic metallosilicate catalysts from waste green container glass*. Ceram. Int. 44, 17069-17073.

ENGELHARDT, G., MICHEL, D., 1987. *High-resolution Solid State NMR of Silicates and Zeolites*. John Wiley & Sons, Chichester, UK.

ESPEJEL-AYALA, F., CHORA CORELLA, R., MORALES PÉREZ, A., PÉREZ-HERNÁNDEZ, R., RAMÍREZ-ZAMORA, R.M., 2014. *Carbon dioxide capture utilizing zeolites synthesized with paper sludge and scrap-glass*. Waste Manage. Res. 32, 1219-1226.

FESTA, R.A., THIELE, D.J., 2011. *Copper: an essential metal in biology*. Curr. Biol. 21, 877-883.

GIRO-PALOMA, J., BARRENECHE, C., MALDONADO-ALAMEDA, A., ROYO, M., FORMOSA, J., INÉS FERNÁNDEZ A., CHIMENOS, J.M., 2019. *Alkali-activated cements for TES materials in buildings' envelops formulated with glass cullet recycling waste and microencapsulated phase change materials*. Materials 12, 2144.

GRAHAM, T.R., DEMBOWSKI, M., MARTINEZ-BAEZ, E., ZHANG, X., JAEGERS, N.R.; HU, J.; GRUSZKIEWICZ, M.S., ET AL., 2018. *In situ ^{27}Al NMR spectroscopy of aluminate in sodium hydroxide solutions above and below saturation with respect to gibbsite*. Inorg. Chem. 57, 11864-11873.

GRBEŠ, A., 2016. *A life cycle assessment of silica sand: comparing the beneficiation processes*. Sustainability 8, 11.

HERIYANTO, PAHLEVANI, F., SAHAJAWALLA, V., 2018. *From waste glass to building materials - An innovative sustainable solution for waste glass*. J. Clean. Prod. 191, 192-206.

HOUSTON, J.R., MAXWELL, R.S., CARROLL, S.A., 2009. *Transformation of meta-stable calcium silicate hydrates to tobermorite: reaction kinetics and molecular structure from XRD and NMR spectroscopy*. Geochem. Trans. 10:1.

IZIDORO, J.D.C., FUNGARO, D.A., ABBOTT, J.E., WANG, S., 2013. *Synthesis of zeolites X and A from fly ashes for cadmium and zinc removal from aqueous solutions in single and binary ion systems*. Fuel 103, 827–834.

JAIN, D., MISHRA, M., RANI, A., 2012. *Synthesis and characterization of novel aminopropylated fly ash catalyst and its beneficial application in base catalysed Knoevenagel condensation reaction*. Fuel Process. Technol. 95, 119-126.

JAISHANKAR, M., TSETEN, T., ANBALAGAN, N., MATHEW, B.B., BEEREGOWDA, K.N., 2014. *Toxicity, mechanism and health effects of some heavy metals*. Interdiscip. Toxicol. 7, 60-72.

JAVADIAN, H., GHORBANI, F., TAYEBI, H.-A., ASL, S.M.H., 2015. *Study of the adsorption of Cd (II) from aqueous solution using zeolite-based geopolymer, synthesized from coal fly ash; kinetic, isotherm and thermodynamic studies*. Arab. J. Chem. 8, 837–849.

JOUHARA, H., KHORDEHGAH, N., ALMAHMOUD, S., DELPECH, B., CHAUHAN, A., TASSOU, S.A., 2018. *Waste heat recovery technologies and applications*. Therm. Sci. Eng. Prog. 6, 268–289.

KUWAHARA, Y., KEITA TSUJI, K., OHMICHI, T., KAMEGAWA, T., MORI, K., YAMASHITA H., 2012. *Waste-slag hydrocalumite and derivatives as heterogeneous base catalysts*. ChemSusChem 5, 1523 – 1532.

LIN, C., WANG, D., YE, S., 2019. *Synthesis of micro-mesoporous glass-analcime composite structure with soda-lime-silica glass as raw material*. Funct. Mater. Lett. 12, 1950021.

MAJDINASAB, A.R., YUAN, Q., 2019a. *Microwave synthesis of zeolites from waste glass cullet using indirect fusion and direct hydrothermal methods: A comparative study*. Ceram. Int. 45, 2400-2410.

MAJDINASAB, A.R., YUAN, Q., 2019b. *Microwave synthesis of zeolites from waste glass cullet using landfill leachate as a novel alternative solvent*. Mater. Chem. Phys. 223, 613-622.

MASHAL, K., HARSH, J.B., FLURY, M., FELMY, A.R. 2005. *Analysis of precipitates from reactions of hyperalkaline solutions with soluble silica*. Appl. Geochem. 20, 1357-1367.

MISHRA, A., 2015. *Impact of silica mining on environment*. J. Geogr. Reg. Plann. 8, 150-156.

NG, E.-P., LIM, G.K., KHOO, G.-L., TAN, K.-H., OOI, B.S., ADAM, F., LING, T.C., WONG, K.-L., 2015. *Synthesis of colloidal stable Linde Type J (LTJ) zeolite nanocrystals from rice husk silica and their catalytic performance in Knoevenagel reaction*. Mater. Chem. Phys. 155, 30-35.

PENA, P., RIVAS MERCURY, J.M., DE AZA, A.H., TURRILLAS, X., SOBRADOS, I., SANZ, J., 2008. *Solid-state ^{27}Al and ^{29}Si NMR characterization of hydrates formed in calcium aluminate-silica fume mixtures*. J. Solid State Chem. 181, 1744-1752.

QIU, W., ZHENG, Y., 2009. *Removal of lead, copper, nickel, cobalt, and zinc from water by a cancrinite-type zeolite synthesized from fly ash*. Chem. Eng. J. 145, 483-488.

RÍOS REYES, C.A., WILLIAMS, C., ALARCÓN, O.M.C., 2013. *Nucleation and growth process of sodalite and cancrinite from kaolinite-rich clay under low-temperature hydrothermal conditions*. Mater. Res. 16, 424-438.

SILVA, R.V., DE BRITO, J., LYE, C.Q., DHIR, R.K., 2017. *The role of glass waste in the production of ceramic-based products and other applications: A review*. J. Clean. Prod. 167, 346-364.

TAKEI, T., OTA, H., DONG, Q., MIURA, A., YONESAKI, Y., KUMADA, N., TAKAHASHI, H., 2012. *Preparation of porous material from waste bottle glass by hydrothermal treatment*. Ceram. Int. 38, 2153–2157.

TAYLOR, J.H., ELMES, V.E., HURT, A.P., COLEMAN, N.J., 2020. *Synthesis of feldspathoids and zeolite K–F from waste amber container glass*. Mater. Chem. Phys. 246, 122805.

TERZANO, R., D'ALESSANDRO, C.; SPAGNUOLA, M., ROMAGNOLI, M., MEDICI, L., 2015. *Facile zeolite synthesis from municipal glass and aluminium solid wastes*. Clean-Soil Air Water 43, 133-140.

VISA, M., CHELARU, A.M., 2014. *Hydrothermally modified fly ash for heavy metals and dyes removal in advanced wastewater treatment*. Appl. Surf. Sci. 303, 14–22.

WANG, Q., LI, J.-S., POON, C.S., 2019. *Recycling of incinerated sewage sludge ash as an adsorbent for heavy metals removal from aqueous solutions*. J. Environ. Manage. 247, 509-517.

XU, B., SMITH, P., WINGATE, C., DE SILVA, L., 2010. *The effect of calcium and temperature on the transformation of sodalite to cancrinite in Bayer digestion*. Hydrometallurgy 105, 75-81.